



HAL
open science

Hybrid Approach for Modeling and Solving of Kinematics of a Compact Bionic Handling Assistant Manipulator

Othman Lakhal, Achille Melingui, Rochdi Merzouki

► **To cite this version:**

Othman Lakhal, Achille Melingui, Rochdi Merzouki. Hybrid Approach for Modeling and Solving of Kinematics of a Compact Bionic Handling Assistant Manipulator. IEEE/ASME Transactions on Mechatronics, 2016, 21 (3), pp.1326 - 1335. 10.1109/TMECH.2015.2490180 . hal-01660738

HAL Id: hal-01660738

<https://hal.science/hal-01660738>

Submitted on 18 Jan 2024

HAL is a multi-disciplinary open access archive for the deposit and dissemination of scientific research documents, whether they are published or not. The documents may come from teaching and research institutions in France or abroad, or from public or private research centers.

L'archive ouverte pluridisciplinaire **HAL**, est destinée au dépôt et à la diffusion de documents scientifiques de niveau recherche, publiés ou non, émanant des établissements d'enseignement et de recherche français ou étrangers, des laboratoires publics ou privés.

Hybrid Approach for Modeling and Solving of Kinematics of Compact Bionic Handling Assistant Manipulator

Othman Lakhal, Achille Melingui, and Rochdi Merzouki

Abstract—This paper deals with a methodology for a real-time solving of a complex kinematics of a class of continuum manipulators, namely the Compact Bionic Handling Assistant (CBHA). First, a quantitative approach is used to model kinematically the CBHA inspired from the modeling of parallel rigid manipulators. For this case, the CBHA is modeled as a series of vertebrae, where each vertebra is connected to the next one through a flexible link. The latter named an inter-vertebra is modeled by a 3UPS-1UP (Universal-Prismatic-Spherical) joints. The kinematic models of the CBHA are derived from the Inverse Kinematic Equations (IKE) of each inter-vertebra. A qualitative approach based on neural networks is used to provide approximated solutions of the IKE for real-time implementation. Thus, the combination of the advantages of quantitative and qualitative approaches allows proposing a hybrid methodology for accurate modeling and solving the kinematics of this class of continuum robots. A set of experiments are conducted using a CBHA in order evaluate the level of efficiency of the proposed hybrid approach.

I. INTRODUCTION

In the last decade, continuum robots have been the subject of intensive research [1]–[4] mainly thanks to their ability to reproduce some biological behaviors such as elephant trunks [5], octopus [6], or tentacles [7]. They are manufactured with flexible materials, allowing them to adapt and maneuver in congested and narrow environments [8]. These properties make them suited for a large number of applications, including surveillance, rescue and exploration.

Continuum robots are often kinematically redundant and highly nonlinear. The lack of sufficient discrete joints renders their kinematic analysis more complex than their rigid-link counterparts. Contributions on kinematic modeling of continuum robots can be distinguished from two approaches: qualitative and quantitative approaches. All of them are based on the available information to describe the robot's behaviors. Qualitative approaches consist of dividing the parametric space into many classes according to the functioning modes. The mathematical and approximative relations between the effects (observation of experts, sensor measurements and statistical data) and causes (input references) are determined using learning techniques. For quantitative approaches, the existing methods are also called model-based methods, which are induced from the physical model (Kinematic, Differential or Dynamic) of the robot in normal functioning mode.

Othman Lakhal and Rochdi Merzouki are with Polytech'Lille, CRISAL, CNRS-UMR 9189, Avenue Paul Langevin, 59655 Villeneuve d'Ascq, France e-mail: othman.lakhal@univ-lille1.fr, achille.melingui@univ-lille1.fr and rochdi.merzouki@polytech-lille.fr

Achille Melingui is with Electrical and Telecommunications Engineering Department of Ecole Nationale Supérieure Polytechnique, the University of Yaoundé I, P. O. Box: 8390 Yaoundé, Cameroon, e-mail: achillemelingui@gmail.com

Regarding model-based methods, various approaches have been proposed for solving the kinematic problem of continuum robots. Hannan et al. [9] used differential geometry and the Denavit-Hartenberg procedure to develop an intuitive kinematic model of a continuum manipulator for planar and spatial scenarios. Generally, this geometrical approach considers the structural assumption of constant curvature of the backbone [10]. Jones and Walker [3] extended this result by considering multiple sections of the manipulator. The same approach was used in [11] to control a flexible endoscopic system, and in [12] to describe the kinematics of a tendon-based manipulator. Godage et al. [13] presented a new three dimensional kinematic model for multi-section continuum arms using a novel shape function-based approach [14], which incorporates geometrically constrained structure of the arm. Another interesting approach is the one presented in [15]; where the authors used torus segments to represent the sections of the Bionic Handling Assistant (BHA) manipulator. Escande et al. [16] developed the forward kinematic model of the Compact Bionic Handling Assistant (CBHA) based on the constant curvature assumption. This singularity can be well handled as studied in [17] and [18]. A geometrical approach to solve the inverse kinematics of continuum robots was proposed and applied to OctArm in [19], where the endpoint for all sections of a multi-section arm are assumed to be known. However, most of the aforementioned modeling techniques lead to less accurate models especially when precision is needed in the robot task, such as handling. In addition, it is often difficult to deduce the inverse kinematics directly from the forward kinematics. Usually, we make use of numerical methods (least squares [20], Newton-Raphson methods [21], etc.) which are computationally intensive.

Concerning qualitative approaches, Giorelli et al. [22] approximated the Inverse Kinematic Model (IKM) of a soft manipulator using a feed-forward Neural Networks (NN). To control a soft extensible manipulator, Braganza et al. [23] used NN to compensate for the dynamic uncertainties. Rolf et al. [2] introduced goal babbling approach to solve the inverse kinematic model of the Bionic Handling Assistant (BHA) robot. Melingui et al. [24] used NN in distal supervised learning scheme to approximate the IKM of the CBHA robot. Then, an adaptive neural network control of the CBHA robot is proposed in [25]. Generally, qualitative approaches lead to more approximate accurately complex models. However, the higher the degree of freedom robots becomes significant (beyond 10 DOF) over the calculation of their kinematic models becomes difficult or long to obtain.

Concerning the modeling of kinematic behaviors of continuum manipulators as a series of parallel robots, Mahl et al. [26] proposed a forward kinematic model of a continuum

robot considering each section as a series of 3-DOF parallel mechanisms. Rongjie et al. [27] solved the problem of multiple solutions of the inverse kinematic model of continuum manipulators using a spline interpolation method. The latter is used to generate the backbone curve of the manipulator assuming that the proximal and distal parts of the continuum manipulator remain straight, and the bends only occur on the middle part of the manipulator. Chirikjian and Burdick [28] developed a modal-approach for hyper-redundant manipulator kinematics. The hyper-redundant manipulators are abstractly represented by backbone curves that either exactly or closely capture the important macroscopic geometric features of the robot. An optimal curve is used to generate the continuous backbone curve. The optimality criteria are used to choose the curve that satisfies task constraints, while optimizing additional criterion. A serial-parallel platforms have been modeled as a basic element of a hyper-redundant robot in Chibani et al [29]. An emulation to the CBHA robot has been produced. Espinoza et al [30] proposed an inverse kinematic modeling for a 10 DOF hyper-redundant robot based on error optimization algorithms.

An alternative to model the kinematic behavior of robots is to combine the two previous approaches in order to take the best of them. In literature, the use of qualitative approaches to improve the performance of quantitative models can be found in [31]–[34], where neural networks were used to approximate a large number of robot manipulator models in presence of nonlinearities. In our previous work, A multilayer neural network has been used in [35] to approximate the solutions of the inverse kinematic equations of the CBHA robot, where the time-allocation for the learning process was considerable, due to the complex kinematic of the robot. A qualitative approach has also been used to approximate the CBHA kinematics [24], [36] and to develop a kinematic controller [25], [37].

Hybrid approach introduced in this paper is an extension of initiated works on CBHA modeling [35] and [25], to a real-time solving in the CBHA modeling is extended in this proposed work by adding a real-time resolution and implementation in case of trajectory tracking. A methodology of kinematic modeling and synthesis of its approximate solutions is proposed for the case of continuum manipulator of type CBHA. The modeling approach is issued from a quantitative modeling of parallel rigid manipulators. Structurally, the CBHA is assimilated to a series of parallel manipulator under the following assumptions: the CBHA's backbone represents a series of vertebrae, an inter-vertebra is modeled as three Universal-Prismatic-Spheric and one Universal-Prismatic (3UPS-1UP) joints, the robot torsion is not considered because the robot is driven at low velocities, also its memory effect of the material. The CBHA's kinematic models are deduced merely from the inverse kinematic equations of each inter-vertebra and generalized for whole the hyper-redundant robot. The obtained inverse kinematic equations are highly nonlinear and mathematically intractable for the CBHA manipulators. For this issue, a multilayer neural network is used to provide approximated solutions of the IKE which can be used for real-time implementation. The advantages of the proposed hybrid modeling-solving approach compared to quantitative methods is that the obtained models are more accurate and compu-

tationally inexpensive. Compared to qualitative approaches, the proposed approach can be implemented for platforms including a significant number of DoFs; because the training database is deduced directly using the inverse kinematic equations. This avoids to operate the robot for a long-period for learning database.

The remainder of the paper is organized as follows: the next Section describes the CBHA manipulator. Section III develops the IKE of the inter-vertebra which is considered as 3UPS-1UP joints. Section IV and Section V present respectively the forward and inverse kinematic modeling of the CBHA using a multilayer neural network for solving the nonlinearity of the inter-vertebra. Section VI describes the obtained experimental results and section VII gives a conclusion and future work.

II. COMPACT BIONIC HANDLING ASSISTANT MANIPULATOR

The CBHA manipulator is mounted on an omnidirectional mobile platform named Robotino. This combination forms a mobile-bionic manipulator called RobotinoXT, as shown in Fig.1.



Fig. 1. RobotinoXT

The CBHA consists of 2 sections made from elastic material, a rotational wrist, and a compliant gripper as depicted in Fig. 2. The key feature of the CBHA is the flexibility of its sections formed by 3 polyamide tubes, controlled by electro-pneumatic actuators. These tubes change their posture when air flow is circulating through them. Since each section is formed by 3 tubes, a bending section can be controlled by applying differential pressures in the tubes. If equal pressures

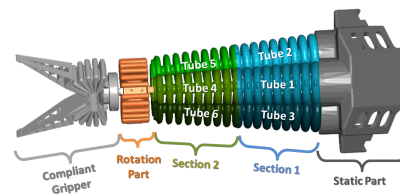


Fig. 2. The CBHA of the RobotinoXT

are applied to each tube, the manipulator extends in a straight line. This extension is limited by an inextensible cable placed in the middle of the backbone, as shown in Fig. 3. The elongations of each tube can be measured from wire-potentiometer sensors placed along each tube. The voltages provided by wire-potentiometer sensors are proportional to the extension of each tube $l_{i,j}$, where $i = 1, \dots, 3$ and $j = 1, 2$ correspond to the wire-potentiometer and section number, respectively. Finally, the CBHA is a class of continuum manipulators, with a continuous

shape and two sections. Each section has 3 DoF of mobility and under actuated.

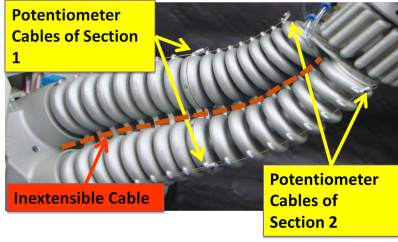


Fig. 3. Length Measurements on the CBHA

III. CBHA MANIPULATOR KINEMATICS

As we have stated in the introduction section, the kinematic behaviors of continuum manipulators can be reproduced under functional and structural assumptions. In this section, the assumptions used for the kinematic modeling are first introduced, and the IKE are derived thereafter.

A. Assumptions

The kinematic models of the CBHA are developed under some assumptions, described below:

- The manipulator is considered as a series of $N = 17$ vertebrae.
- An inter-vertebra is flexible and non deformable with a 3DoF mobility. It is modeled with a 3UPS-1UP joints.
- The manipulator's yaw motion is not allowed with the existing mechanical links between the tubes.

Based on these assumptions, a parallel robot composed by two rigid platforms and 3 DoF of mobility is used to emulate the behavior of each inter-vertebra. Knowing that the robot comprises 17 vertebrae, the entire CBHA can be emulated by a series of 16 parallel robots each comprising 3 DoF. Using such modeling, CBHA can be considered as a 48 DoF system. That is why the CBHA robot has the properties of hyper-redundant robots. The schema of an inter-vertebra is given in Fig. 4. It consists of a lower and a upper vertebrae connected by three limbs with identical kinematic configuration, and a central leg. The limbs are modeled by a kinematic configuration of type UPS, in which only the prismatic joints are active allowing to control the position and orientation of the upper vertebra relative to the lower vertebra. $q_{m,k}$ represents the variation of length of prismatic joint, where $m = 1, \dots, 3$ is the number of active joints and $k = 1, \dots, N - 1$ is the number of inter-vertebrae. The central leg is modeled by a kinematic configuration of type PU located in the center of an inter-vertebra. It is considered as a passive joint.

B. Inverse Kinematic Equation of the CBHA's Inter-Vertebra

The IKEs of an inter-vertebra are obtained by calculating the joint variables $q_{m,k}$ corresponding to the pose (position and orientation) of the upper vertebra's centre relative to the lower vertebra frame. In the case of CBHA manipulator, the inter-vertebra is considered as a 3-DoF parallel robot, because of

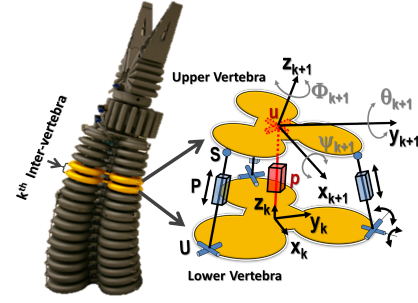


Fig. 4. Schematic of an inter-vertebra modeled as parallel robot with 3UPS-1UP

movements constraints related to the passive kinematic chain UP. In fact, the rotation with respect to the z axis, denoted by $Rot(z, \Phi_k)$, and the translations relative to the x and y axes denoted by $Trans(x, X_k)$ and $Trans(y, Y_k)$, respectively, are not considered, because it does not exist a movement on these axis. Only the translation along the z axis is possible which is denoted by $Trans(z, Z_k)$. Hence, the IKEs can be formulated as follows:

$$q_{m,k} = f(Z_k, \psi_k, \theta_k) \quad (1)$$

where the angles θ_k and ψ_k indicate pitch and roll angles, respectively.

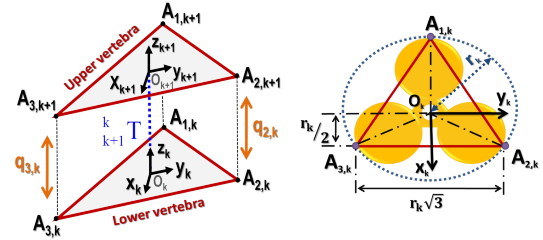


Fig. 5. Configuration of spatial 3UPS-1UP manipulator

$A_{m,k}$ represents the connection point between the extensible driving leg $m = 1, \dots, 3$ and the vertebra $k = 1, \dots, N - 1$, as shows the Fig 5. For each vertebra, the points $A_{1,k} A_{2,k} A_{3,k}$ form an equilateral triangle. The frame $\mathcal{R}_{k+1} \{O_{k+1}, x_{k+1}, y_{k+1}, z_{k+1}\}$ is attached to the upper vertebra of origin O_{k+1} , located at the centre of the equilateral triangle $A_{1,k+1}A_{2,k+1}A_{3,k+1}$, and the frame $\mathcal{R}_k \{O_k, x_k, y_k, z_k\}$ is attached to the lower vertebra of origin O_k , centre of the triangle $A_{1,k}A_{2,k}A_{3,k}$. Knowing that the entire shape of the CBHA is conical, it is necessary to determine the circumcircle radius r_n of the considered vertebra, where $n = 1, \dots, N$ is the number of vertebrae. Let r_{max} and r_{min} , respectively the radius of the base and the apex of the backbone, the radius of each vertebra r_n can be calculated by:

$$r_n = \frac{k}{N}(r_{min} - r_{max}) + r_{max} \quad (2)$$

where $N = 17$ is the number of vertebrae. Thus, the coordinates of the three connection points are given by the coordinates (3), relative to the centre of the n^{th} vertebra.

$$A_{1,k} = \begin{bmatrix} -r_k \\ 0 \\ 0 \end{bmatrix}; A_{2,k} = \begin{bmatrix} \frac{1}{2}r_k \\ \frac{\sqrt{3}}{2}r_k \\ 0 \end{bmatrix}; A_{3,k} = \begin{bmatrix} \frac{1}{2}r_k \\ -\frac{\sqrt{3}}{2}r_k \\ 0 \end{bmatrix}. \quad (3)$$

The length of the prismatic joint for the active kinematic chain of each UPS is represented by: $q_{m,k}$ with $m = 1, \dots, 3$ and $k = 1, \dots, N - 1$. The coordinates of the connection point $A_{m,k+1}$ relative to the frame $A_{m,k}$ are given as follows:

$$\begin{bmatrix} Q_{m,k} \\ 1 \end{bmatrix} = {}_{k+1}^k T \begin{bmatrix} A_{m,k+1} \\ 1 \end{bmatrix} - \begin{bmatrix} A_{m,k} \\ 1 \end{bmatrix} \quad (4)$$

where, ${}_{k+1}^k T$ is the transformation matrix of the upper vertebra frame relative to the lower vertebra. $Q_{m,k}$ is 3x1 vector like $A_{m,k+1}$.

$${}_{k+1}^k T = \begin{pmatrix} C\theta_k & S\theta_k S\psi_k & S\theta_k C\psi_k & 0 \\ 0 & C\psi_k & -S\psi_k & 0 \\ -S\theta_k & S\psi_k C\theta_k & C\theta_k C\psi_k & Z_k \\ 0 & 0 & 0 & 1 \end{pmatrix}. \quad (5)$$

The notations C and S mean cosine and sine functions, respectively. Thus, the prismatic variable $q_{m,k}$ is equal to the distance between the connection points $A_{m,k+1}$ and $A_{m,k}$:

$$q_{m,k}^2 = Q_{m,k}^T Q_{m,k} \quad (6)$$

Therefore, after introducing of (3) into (4), the equation (6) can be rewritten in the format of (1):

$$q_{1,k} = \text{sqr}t \left(Z_k^2 + 2Z_k r_{k+1} S\theta_k - 2r_{k+1} r_k C\theta_k + r_{k+1}^2 + r_k^2 \right), \quad (7)$$

$$q_{2,k} = \text{sqr}t \left(Z_k^2 + Z_k r_{k+1} (\sqrt{3}C\theta_k S\psi_k - S\theta_k) - r_{k+1} r_k \left(\frac{\sqrt{3}}{2} S\theta_k S\psi_k + \frac{3}{2} C\psi_k + \frac{1}{2} C\theta_k \right) + r_{k+1}^2 + r_k^2 \right), \quad (8)$$

$$q_{3,k} = \text{sqr}t \left(Z_k^2 - Z_k r_{k+1} (\sqrt{3}C\theta_k S\psi_k + S\theta_k) + r_{k+1} r_k \left(\frac{\sqrt{3}}{2} S\theta_k S\psi_k - \frac{3}{2} C\psi_k - \frac{1}{2} C\theta_k \right) + r_{k+1}^2 + r_k^2 \right). \quad (9)$$

IV. FORWARD KINEMATIC MODEL OF THE CBHA

In this section, the Forward Kinematic Model (FKM) of an inter-vertebra is first derived from the IKE using neural networks approximation. The FKM of the entire CBHA's backbone is deduced thereafter.

A. Forward Kinematic Model of the CBHA's inter-vertebra

The relation between the joint configuration $q_{m,k}$ of an inter-vertebra and the parameters of the upper-vertebra (Z_k , θ_k , and ψ_k) relative to the lower vertebra frame is the FKM of the parallel robot module 3UPS-1UP, defined as:

$$[Z_k, \theta_k, \psi_k] = f^{-1}(q_{m,k}). \quad (10)$$

The pose $[Z_k, \theta_k, \psi_k]$ of the upper vertebra frame corresponding to a particular joint configuration $q_{m,k}$ relative to the lower vertebra frame can be obtained by solving the IKEs ((7), (8), and (9)). However, as we can notice, these equations are highly nonlinear. Numerical techniques such as

least square, Newton-Raphson methods [38] which are used to provide approximated solutions are usually computationally intensive. In this work, an approximated solution is provided by a Multilayer Neural Network (MNN). The approximation of the solution can be summarized to a regression problem with non-noisy data, because the IKEs are supposed to be well identified.

Neural Network (NN) is a technique that models mechanisms based on learning and problem solving functions of the human brain. NNs possess many useful properties and capabilities [39] in terms of nonlinearity approximation, input-output mapping, adaptive controlling, very-large-scale integration, implementability, etc. In NN model, the signals flow consecutively through the different layers from the input to the output layer. The intermediary layers are called hidden layers. In each layer, each elementary unit calculates a scalar product between a vector of weights and the output vector given by the previous layer. The choice of the appropriate network architecture (i.e. number of hidden layers, number of nodes in each layer, activation function, etc.) has to be identified during the training process [39]. After the choice of the NN architecture, the values of the weights are adjusted via the training process (back-propagation, delta rule, etc.). The performance of the obtained model is closely related to the type and quality of the input-output data pairs, and noisy data can significantly degrade its performance.

Multilayer Perceptron (MLP) is one of the typical examples of Artificial NNs and consists of an input layer, some hidden layers, and an output layer. NNs are considered as "universal approximators"; Hornik et al. [40] proved that an MLP with two layers of weights and sigmoid activation functions can approximate any nonlinear functional relationship (mapping) with an arbitrary accuracy, provided that enough of hidden neurons are available. The solution of the IKEs based on NN approximation offers advantages such as reduced computational resources and rapid execution for real-time purposes.

In this work, each bending section of the CBHA is divided into a finite number of inter-vertebrae. However, the measurement of the length of each inter-vertebra increases the implementation cost. Ideally for the case of the CBHA, the measurement of the length of each inter-vertebra requires 48 length sensors for each section, 92 length sensors for the entire CBHA's backbone. An alternative is to fragment, when possible the wire-cable length sensor to provide the length of each parallel platform module. A fragmentation based on the minimum potential energy approximation has been proposed in [41] for the BHA robot. However, the latter is still based on assumptions: disregard of the potential energy due to gravitation, potential energy of the trunk is equal to energy stored in its spring-like bellows actuators, which are not always verified. Referred to CBHA, the length of each inter-vertebra is different due to tapered structure of the CBHA, with tilted position on the mobile platform (Robotino). However, since the length of an inter-vertebra is a fraction of the tube length, the elongation of each inter-vertebra at any time represents a percentage of the total length of the tube. This percentage can be obtained by considering the minimum and the maximum elongations of each inter-vertebra listed in

Table I. The first and the fourth rows represent the index of the vertebra. The second and the fifth rows give the minimum elongations, while the third and the sixth give maximum elongations. The percentage distribution of the inter-vertebra's length for the entire CBHA is depicted in Fig. 6.

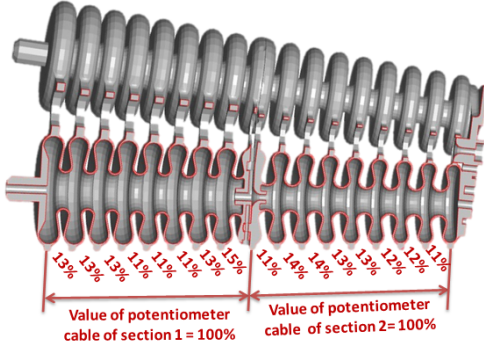


Fig. 6. Elongation of the inter-vertebrae during movement

For FKM modeling, each section of the CBHA is modeled by one NN model of 24-inputs to 24-outputs. The lengths of the inter-vertebrae ($q_{1,k}, q_{2,k}, q_{3,k}$) are considered as inputs, while the variable Z_k , the pitch (θ_k), and the yaw (ψ_k) angles are considered as outputs. $k = 1, 2, \dots, 8$ for the first section, and $k = 9, 10, \dots, 16$ for the second sections.

TABLE I
LIMIT ELONGATION OF k^{th} INTER-VERTEBRA IN MILLIMETER FOR THE CASE OF CBHA

k^{th}	1	2	3	4	5	6	7	8
q_{min} (mm)	8.5	8.5	8.5	7	7	7	8.5	10
q_{max} (mm)	19.5	19.5	19.5	16.5	16.5	16.5	20	22
k^{th}	9	10	11	12	13	14	15	16
q_{min} (mm)	6.5	8	8	7.5	7.5	7	7	6.5
q_{max} (mm)	16	20.5	20.5	19	19	18	18	16

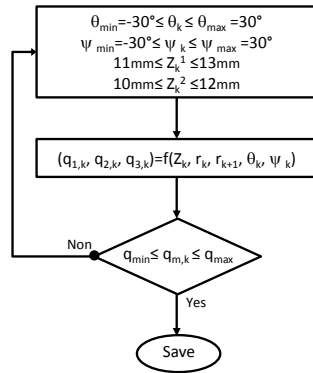


Fig. 7. Database of learning generation

As it is listed in Table I, each inter-vertebra length is bounded. These bounds allow fixing the range of the pitch (θ_k) and the yaw (ψ_k) angles. In fact, the variables Z_k , θ_k , and ψ_k are initialized with a large range, as shown in Fig.7. According to Fig. 7, the IKEs are computed, and the samples of input-output pairs included in the range of the lengths of

the inter-vertebrae ($q_{1,k}, q_{2,k}, q_{3,k}$) are saved. A learning base of 30071 samples is obtained; 11559 samples for the first section and 18512 samples for the second section, respectively. The learning base is divided randomly: 70% for the training set, 15% for the validation set, and 15% for the test set. The training set is used during the learning phase and the test set is only employed to assess the performance of the neural network model. The validation set is used during the learning phase.

In order to minimize the Mean Square Error (MSE) calculated in the validation set, the weight matrices are adjusted by means of the back-propagation descent method, including the momentum term. For an optimal generalization of neural network models and to avoid over-fitting, the early-stopping method for training is implemented. The latter requires that after a period of training (epochs) using the training set, the weight matrices of the NN are fixed, and the NN operates in the forward mode using the validation set. The process is repeated until the MSE on the validation set reaches its minimum value. In order to empirically select the best model for each regressors, the value of each parameter was varied in a given predefined range according to a grid search over the learning base. A MLP of two layers is used for each CBHA's section, and it is tested with 2 up to 20 neurons (with a step of 2 neurons) in each hidden layer. The optimal MLP architecture is obtained for an architecture with 18 neurons in each hidden layer for the two sections by taking the MSE in the validation set as a performance criterion. The assessment of the trained MLP in terms of MSE on the test-samples yields the values reported in Table II.

TABLE II
RESULTS ACHIEVED BY EACH NEURAL NETWORK MODEL ON THE TEST SAMPLES

Neural networks topologies	Neurons	MSE
MLP, section 1 (2 layers)	18	$6.4612 \cdot 10^{-5}$
MLP, section 2 (2 layers)	18	$8.2425 \cdot 10^{-5}$

In the view of the obtained performance, we notice that each NN model approximates the variables Z_k , θ_k , and ψ_k with a good degree of accuracy. In next subsection, the FKM of the entire CBHA is deduced.

B. FKM of the CBHA manipulator

Fig. 8 depicts the different frames used to describe the kinematics of the CBHA:

- The first frame $\{X_{base}, Y_{base}, Z_{base}\}$ is attached to the base of the CBHA robot;
- The second frame $\{X_{s1}, Y_{s1}, Z_{s1}\}$ is attached to the top of the first bending section;
- And the last one $\{X_{s2}, Y_{s2}, Z_{s2}\}$ is attached to the top of the second bending section;

The coordinates of the frames $\{X_{s1}, Y_{s1}, Z_{s1}\}$ and $\{X_t, Y_t, Z_t\}$ are given relative to the base frame $\{X_{base}, Y_{base}, Z_{base}\}$, while those of the frame $\{X_{s2}, Y_{s2}, Z_{s2}\}$ are expressed relative to frame $\{X_{s1}, Y_{s1}, Z_{s1}\}$.

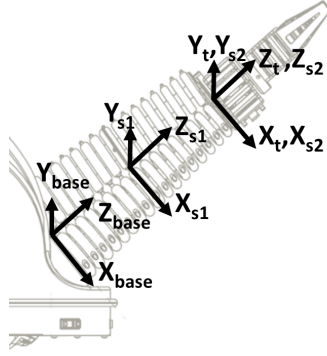


Fig. 8. The associated frames of the CBHA

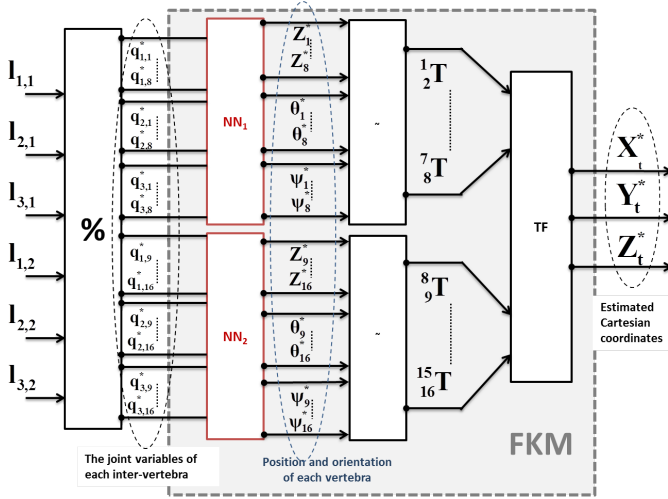


Fig. 9. Forward kinematic algorithm

The modeling process of the FKM is summarized in Fig. 9. The lengths provide by the tube-length's sensors are divided with respect of the percentage distribution of the inter-vertebrae. The elongations $q_{m,k}$ obtained are used as inputs of the NN models. NN1 model provides the predicted pose of the vertebrae of the first section, while those of the second section are provided by NN2 model. The Cartesian coordinate of the tip arm $\{X_t, Y_t, Z_t\}$ is obtained by using the transformation matrices ${}^k_{k+1}T$, for $k = 1, \dots, N - 1$.

V. INVERSE KINEMATIC MODEL OF THE CBHA

In this section, the IKM of the CBHA is presented. As we stated at Section III, the entire CBHA is emulated by a series of 16 parallel robots each comprising 3 DoF. Using such modeling, the CBHA can be considered as a 48 DoF manipulator. Numerically, it is sufficient to calculate the IKM of each vertebra system, making the relation between the center of the upper-platform with the joint coordinates of the inter-vertebra. It comes more complicated for deducing the numerical relationship between the top of the CBHA and the 48 joint coordinates. Based on the approximation and generalization capabilities of the learning-based techniques the IKM can be solved. The principle is to compute the

corresponding lengths of each inter-vertebra from a given Tool Center Position (TCP). At the end, the IKM of the CBHA is obtained by summing the elongations of the inter-vertebrae.

In contrast to FKM, four MLPs are used to approximate the IKM of the CBHA. The first one approximates the end-position $\{X_{s1}, Y_{s1}, Z_{s1}\}$ of the first section from the Cartesian coordinates of the CBHA's tip $\{X_t, Y_t, Z_t\}$. The last three models use the position of the arm's tip $\{X_t, Y_t, Z_t\}$ and the end-position of the first section $\{X_{s1}, Y_{s1}, Z_{s1}\}$ as inputs, and provides Z_k, θ_k , and ψ_k as outputs.

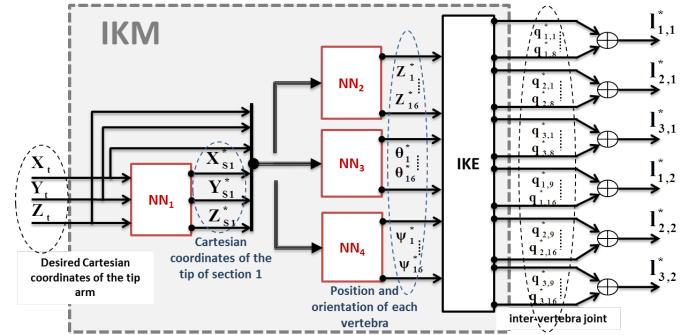


Fig. 10. Algorithm for Inverse kinematic modeling

Fig.10 summarizes the process of the IKM solving. The same learning base developed for the Forward kinematics is used to derive the inverse kinematics. Table III shows the results achieved by each neural network model on the test set samples. The performance is less accurate for the end-position of the first section. This is mainly due to CBHA hyper-redundancy, because many solutions of the CBHA's tip are possible for the same end-position of the first section. Nevertheless, the performance achieved remains acceptable. To select a particular inverse kinematics function, a squared penalty term is added to the objective function of the neural network. The cost functional yields:

$$J = \frac{1}{2} (X_d - X)^T (X_d - X) + \lambda \frac{1}{2} \|X\|^2 \quad (11)$$

where X and X_d are respectively the predicted and the desired position. $\|\cdot\|$ denotes the Euclidean norm. In [42], it has been demonstrated that, if the coefficient λ is larger, X becomes small. The penalty term λ provides a possibility to control efficiency the magnitude of X . This allows selecting a particular inverse solution.

TABLE III
RESULTS ACHIEVED BY EACH NEURAL NETWORK MODEL ON THE TEST SAMPLES

Neural networks topologies	Neurons	MSE
MLP, NN1 (2 layers)	18	$4.9840 \cdot 10^{-4}$
MLP, NN2 (2 layers)	12	$1.2363 \cdot 10^{-5}$
MLP, NN3 (2 layers)	16	$4.0503 \cdot 10^{-5}$
MLP, NN4 (2 layers)	16	$3.4651 \cdot 10^{-5}$

The whole MSE listed in Table III and Table II are the errors obtained on the test samples. The database has been divided in three sets: training, validation, and test. During the NN

training, the matrices are updated using the MSE calculated at the same stage. MSE in validation set is used for stopping the training, and the MSE in the test set is used for assessing the performance of the NN model.

VI. EXPERIMENTAL RESULTS

This section focuses on the validation of the developed kinematic models. Regarding the comparative study, performances of modeling approaches vary from one robot to another [2], [22], [23], [43], [44]. They depend on the structure of the continuum manipulator, the state of its actuators, and its geometry (sizes, shape). Hence, a direct comparison of these approaches can be done, if and only if the latter can be implemented on the same manipulator. This paper discusses only recent contributions done on the CBHA and the BHA manipulators. The structure is almost the same, the difference being that the CBHA possesses two sections, while the BHA has three sections. In this section, the optical 3-D stereo-vision system is first presented for the real-time trajectory tracking. The validations of the FKM and IKM are presented thereafter. The section ends with a discussion.

A. Trajectory Generation

For generating the trajectory of the CBHA's tip, three reflective markers are attached to each head of its two sections. The reflective markers are tracked by a stereo-vision system in order to reconstruct the trajectory generated by each head. The desired trajectory of the tip of the manipulator is generated by pressure variation. The process of the trajectory tracking is presented in Fig. 11. The trajectory generated by the head of the second CBHA's section is considered as desired trajectory.

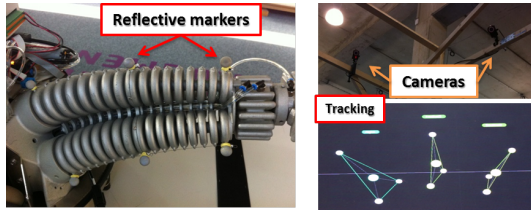


Fig. 11. Stereo-vision system for trajectory generation

The tracking set-up is based on the motion capture system OptiTrack by NaturalPoint, and consists of a set of 10 infrared cameras capable of an accurate 3D tracking of a point cloud within their combined visible workspace, in our case approximately a cube of 1 meter side. After calibration, the system has a precision of 0.3 mm for measuring the 3D displacements of the two sections, as well as the base point considered as the inertial frame of the system. The system has already been used in [45].

B. Validation of the forward kinematic model of the CBHA.

The forward kinematics of the CBHA are validated by following the experimental setup presented in Fig. 12. The desired posture of the CBHA is generated by applying a

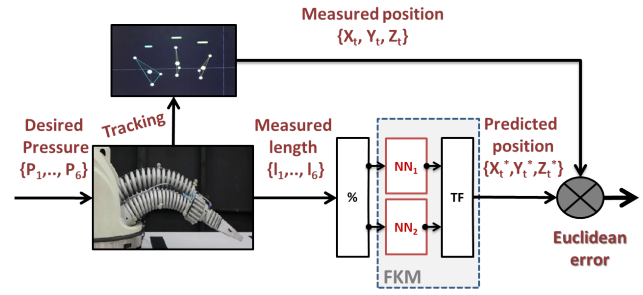


Fig. 12. Architecture of the FKM validation

set of the desired pressures to CBHA's tubes. During the trunk displacements, the values provided by the length sensors are used as inputs to the FKM. The predicted positions are compared to those provided by the stereo-vision system. Results of the FKM validation are represented in Fig. 13. The trajectories generated by the FKM and the stereo-vision system are depicted in Fig. 13 (a). The associated Euclidean errors are represented in Fig. 13-(b)-(c)-(d).

Refer to Euclidean errors presented in Fig. 13, it can be concluded that the proposed FKM is able to predict the CBHA's tip pose with positioning errors of less than 8mm.

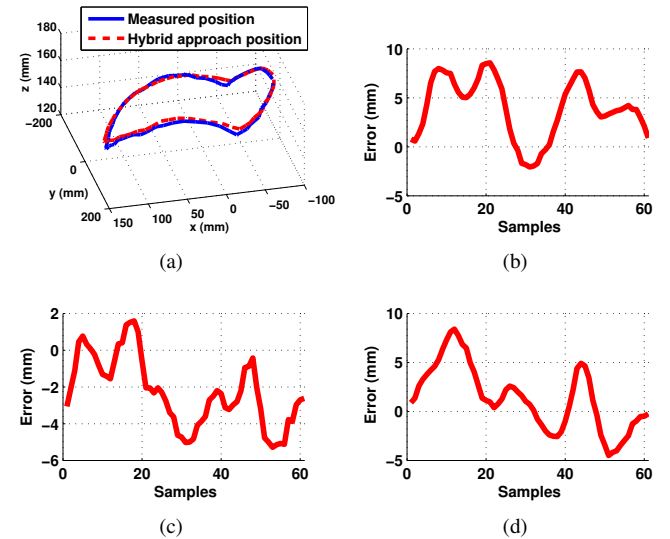


Fig. 13. Kinematic Validation: (a) Desired and Estimated trajectories; (b) Euclidean error in X axis; (c) Euclidean error in Y axis; and (d) Euclidean error in Z axis.

C. Validation of the inverse kinematics of the CBHA

The validation of the inverse CBHA's kinematics is proceeded as shown on Fig. 14. The desired posture of the CBHA is generated by applying a set of the desired pressures to CBHA's tubes. The desired positions of CBHA's tip is applied to IKM, and the predicted lengths generated by the IKM are used as input to length-pressure controller. The pressures generated by the controller are applied to CBHA robot by mean of the internal PID controllers. The elongations

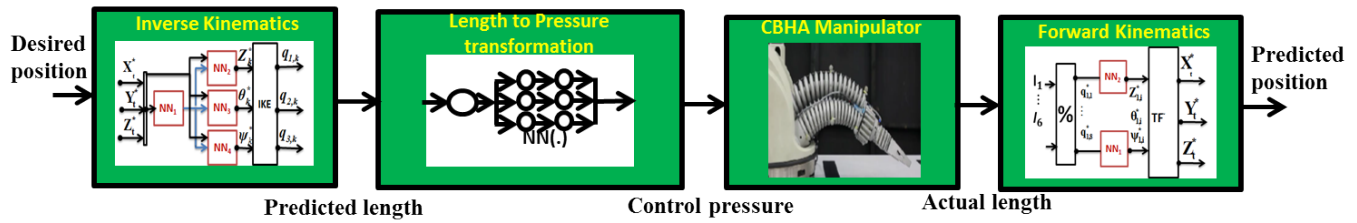


Fig. 14. Architecture of the kinematic models validation

provided by the length sensors are used as inputs to FKM. The outputs of the FKM constitute the predicted positions. These positions are compared to those provided by the stereo vision system. Note that the CBHA system embeds six internal PID controllers allowing the control of the pressure in each tube. The length-pressure controller has been developed in our previous works [37].

Fig. 15 presents the results achieved by the IKM. Fig.15-(a) depicts the trajectories of the IKM and the stereo vision system. Fig. 15-(b)-(c)-(d) represent the associated Euclidean errors. Euclidean errors in Fig. 15 conclude that the proposed IKM is able to predict the CBHA's lengths which lead to tip pose with positioning errors less than 11 mm. The posture

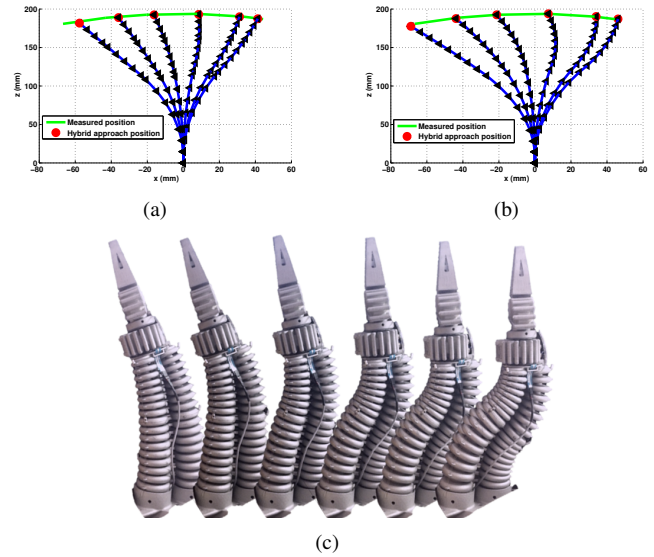


Fig. 16. Posture of the CBHA: (a) Estimated posture with the IKM ; (b) Estimated posture with the FKM; and (c) real posture of the CBHA.

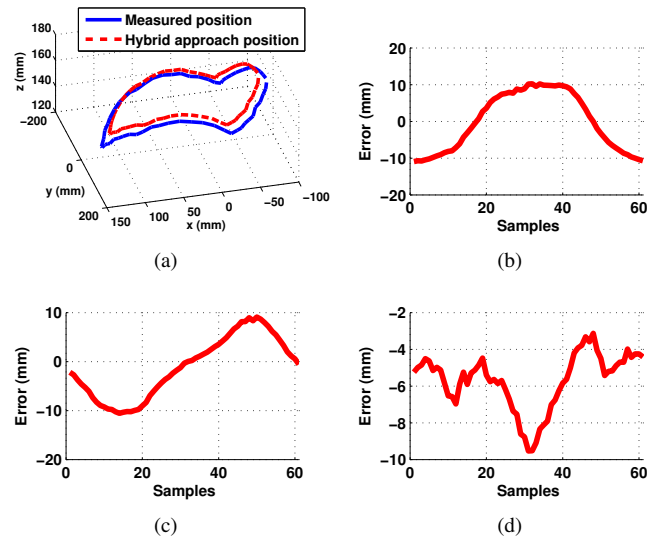


Fig. 15. Inverse kinematic Validation: (a) Desired and IKM trajectories; (b) Euclidean error in X axis; (c) Euclidean error in Y axis; and (d) Euclidean error in Z axis.

of the CBHA can also be deduced from the positions and orientations of the vertebrae, as shown in Fig. 16. The predicted CBHA's postures obtained by using the IKM and FKM models are represented in Fig. 16-(a)-(b). The real CBHA's posture obtained by using the values provided by the length sensors is represented in 16 (c). We notice that both predicted CBHA's postures are closed to the real CBHA's posture, and those obtained by FKM function are the closest.

D. Discussions

In the view of the obtained results, the proposed kinematic models achieve good performance. The proposed FKM is able

to predict the CBHA's tip pose with positioning errors of less than 8mm, which represents 2.2% of the total length of the CBHA. The IKM predicts the CBHA's lengths which lead to the tip pose with positioning errors of less than 11mm, which represents 3% of the total length of the CBHA. The CBHA includes memory effects and non-stationary behaviors due to trunk's materials (polyamide). When the CBHA's trunk spends long time in bending-posture, it does not return to its initial posture when it is released. These non-stationary behaviors appear mainly in high CBHA dynamics, and cannot be coped by a simple kinematic controller [37]. Remaining models' errors are expected to result from torsional effects which have been neglected in modeling process. Table IV lists recent contributions in kinematic modeling of continuum robots. We notice that in the case of the CBHA modeling and real-time implementation, learning-based methods achieve good performance, while quantitative methods are less accurate. This lack of performance should result from modeling assumptions inherent in quantitative approaches. The proposed hybrid approach is intermediary to previous approaches, and shows average performance. The accuracy of tracking tasks by the CBHA is shown through the video [46], for online targets tracking. These targets correspond to the centre of tool coordinates of an external rigid robot manipulator which can communicate with the CBHA through the network inside the

TABLE IV
RECENT CONTRIBUTIONS IN KINEMATIC MODELING OF CBHA AND BHA ROBOT

Robots	Characteristics	Modeling Method	Kinematic modeling
CBHA	Continuous Shape, Structure: Soft, 2 sections, 3 tubes per section, 17 vertebrae, 3 DoF per inter-vertebra, Pneumatic actuation, Length: 0.50 m.	Hybrid approach: Geometry and Neural Network, Proposed approach	Forward (FKM), accuracy: 8 mm; Inverse (IKM), accuracy: 11 mm; Validation: Simulation and real-time experiments.
		Quantitative: Geometrical-based approach Escande et al. [43]	Forward (FKM), accuracy: 8 mm; Validation: Simulation and real-time experiments.
		Qualitative: Neural Network, Melingui et al. [24], [36]	Forward (FKM), accuracy: 4 mm; Inverse (IKM), accuracy: 5 mm; Validation: Simulation and real-time experiments.
BHA	Continuous shape, Structure: Soft, 3 sections, 3 tubes per section, Pneumatic actuation, 30 vertebrae, 3 DoF per inter-vertebra, Length: 1.00 m	Quantitative: Geometrical-based approach, Mahl et al. [41]	Forward (FKM), accuracy: 20 mm, Inverse (IKM), accuracy: 50 mm, Validation: Simulation and real-time experiments
		Qualitative: Goal babbling learning, Rolf et al. [2]	Forward (FKM), accuracy: 5 mm; Inverse (IKM), accuracy: 6 mm; Validation: Simulation and real-time experiments.

CBHA's workspace. The aim is that the rigid manipulator transfers to the CBHA the coordinates of its centre of tool at the end of each trajectory, calculated in the local CBHA's frame. Then, the CBHA free-load tracks the imposed target with a good accuracy.

VII. CONCLUSIONS

In this paper, we presented a methodology of kinematic modeling calculation of a class of continuum manipulator, including its approximate modeling for real-time solving and implementation. The proposed modeling approach is able to model hyper-redundant or continuum manipulators that consist of multiple bending sections. The difficulty of solving the inverse kinematic equations is circumvented by providing approximated solutions based on neural network approach. Both the forward and inverse kinematics are derived from the inverse kinematic equations. The obtained kinematic models are computationally inexpensive and can be easily implemented in real-time. They can reconstruct the tool center position of a free load CBHA with an interesting degree of accuracy. The validation of the kinematic models using a 3-D stereo vision system for trajectory tracking demonstrate the efficiency of the proposed modeling approach. In future work, dynamic behaviors of the CBHA in interaction with external environment can be considered for control purpose.

REFERENCES

- [1] I. D. Walker, "Robot strings: long, thin continuum robots," in *Aerospace Conference, 2013 IEEE*. IEEE, 2013, pp. 1–12.
- [2] M. Rolf and J. J. Steil, "Efficient exploratory learning of inverse kinematics on a bionic elephant trunk," 2012.
- [3] B. A. Jones and I. D. Walker, "Kinematics for multisection continuum robots," *Robotics, IEEE Transactions on*, vol. 22, no. 1, pp. 43–55, 2006.
- [4] G. Robinson and J. B. C. Davies, "Continuum robots-a state of the art," in *Robotics and Automation, 1999. Proceedings. 1999 IEEE International Conference on*, vol. 4. IEEE, 1999, pp. 2849–2854.
- [5] R. Behrens, M. Poggendorf, E. Schulenburg, and N. Elkmann, "An elephant's trunk-inspired robotic arm - trajectory determination and control," in *Robotics; Proceedings of ROBOTIK 2012; 7th German Conference on*. VDE, 2012, pp. 1–5.
- [6] M. Sfakiotakis, A. Kazakidi, N. Pateromichelakis, and D. P. Tsakiris, "Octopus-inspired eight-arm robotic swimming by sculling movements," in *Robotics and Automation (ICRA), 2013 IEEE International Conference on*. IEEE, 2013, pp. 5155–5161.
- [7] H. Martinez-Alfaro and S. Gomez-Garcia, "Mobile robot path planning and tracking using simulated annealing and fuzzy logic control," *Expert Systems with Applications*, vol. 15, no. 3, pp. 421–429, 1998.
- [8] I. D. Walker, D. M. Dawson, T. Flash, F. W. Grasso, R. T. Hanlon, B. Hochner, W. M. Kier, C. C. Pagano, C. D. Rahn, and Q. M. Zhang, "Continuum robot arms inspired by cephalopods," in *Defense and Security*. International Society for Optics and Photonics, 2005, pp. 303–314.
- [9] M. Hannan and I. Walker, "Novel kinematics for continuum robots," in *Advances in Robot Kinematics*. Springer, 2000, pp. 227–238.
- [10] R. J. Webster and B. A. Jones, "Design and kinematic modeling of constant curvature continuum robots: A review," *The International Journal of Robotics Research*, vol. 29, no. 13, pp. 1661–1683, 2010.
- [11] B. Bardou, P. Zanne, F. Nageotte, and M. de Mathelin, "Control of a multiple sections flexible endoscopic system," in *Intelligent Robots and Systems (IROS), 2010 IEEE/RSJ International Conference on*. IEEE, 2010, pp. 2345–2350.
- [12] Q. Zhao and F. Gao, "Design and analysis of a kind of biomimetic continuum robot," in *Robotics and Biomimetics (ROBIO), 2010 IEEE International Conference on*. IEEE, 2010, pp. 1316–1320.
- [13] I. S. Godage, E. Guglielmino, D. T. Branson, G. A. Medrano-Cerda, and D. G. Caldwell, "Novel modal approach for kinematics of multisection continuum arms," in *Intelligent Robots and Systems (IROS), 2011 IEEE/RSJ International Conference on*. IEEE, 2011, pp. 1093–1098.
- [14] I. S. Godage, D. T. Branson, E. Guglielmino, G. A. Medrano-Cerda, and D. G. Caldwell, "Shape function-based kinematics and dynamics for variable length continuum robotic arms," in *Robotics and Automation (ICRA), 2011 IEEE International Conference on*. IEEE, 2011, pp. 452–457.

- [15] M. Rolf and J. J. Steil, "Constant curvature continuum kinematics as fast approximate model for the bionic handling assistant," in *Intelligent Robots and Systems (IROS), 2012 IEEE/RSJ International Conference on*. IEEE, 2012, pp. 3440–3446.
- [16] C. Escande, R. Merzouki, P. M. Pathak, and V. Coelen, "Geometric modelling of multisection bionic manipulator: Experimental validation on robotinoxt," *IEEE International Conference on Robotics and Biomimetics (ROBIO)*, December 2012.
- [17] A. Reiter, A. Bajo, K. Iliopoulos, N. Simaan, and P. K. Allen, "Learning-based configuration estimation of a multi-segment continuum robot," in *Biomedical Robotics and Biomechanics (BioRob), 2012 4th IEEE RAS & EMBS International Conference on, IEEE, 2012*, pp. 829–834.
- [18] W. Wei, R. E. Goldman, H. F. Fine, S. Chang, and N. Simaan, "Performance evaluation for multi-arm manipulation of hollow suspended organs," *Robotics, IEEE Transactions on*, vol. 25, no. 1, pp. 147–157, 2009.
- [19] S. Neppalli, M. A. Csencsits, B. A. Jones, and I. Walker, "A geometrical approach to inverse kinematics for continuum manipulators," in *Intelligent Robots and Systems, 2008. IROS 2008. IEEE/RSJ International Conference on*. IEEE, 2008, pp. 3565–3570.
- [20] J. M. Hollerbach and C. W. Wampler, "The calibration index and taxonomy for robot kinematic calibration methods," *The international journal of robotics research*, vol. 15, no. 6, pp. 573–591, 1996.
- [21] A. Goldenberg, B. Benhabib, R. G. Fenton *et al.*, "A complete generalized solution to the inverse kinematics of robots," *Robotics and Automation, IEEE Journal of*, vol. 1, no. 1, pp. 14–20, 1985.
- [22] M. Giorelli, F. Renda, G. Ferri, and C. Laschi, "A feed-forward neural network learning the inverse kinetics of a soft cable-driven manipulator moving in three-dimensional space," in *proc. IEEE Int. Conf. on Intelligent Robots and Systems*, pp. 5033–5039, 2013.
- [23] D. Braganza, D. M. Dawson, I. D. Walker, and N. Nath, "A neural network controller for continuum robots," *Robotics, IEEE Transactions on*, vol. 23, no. 6, pp. 1270–1277, 2007.
- [24] A. Melingui, R. Merzouki, J. Mbede, C. Escande, B. Daachi, and N. Benoudjit, "Qualitative approach for inverse kinematic modeling of a compact bionic handling assistant trunk," in *Neural Networks (IJCNN), 2014 International Joint Conference on*. IEEE, 2014, pp. 754–761.
- [25] A. Melingui, O. Lakhal, B. Daachi, J. B. Mbede, and R. Merzouki, "Adaptive neural network control of a compact bionic handling arm," *IEEE/ASME Transactions on Mechatronics, Issue: 99 DOI: 10.1109/TMECH.2015.2396114*, Mars 2015.
- [26] T. Mahl, A. Hildebrandt, and O. Sawodny, "Forward kinematics of a compliant pneumatically actuated redundant manipulator," in *Industrial Electronics and Applications (ICIEA), 2012 7th IEEE Conference on*. IEEE, 2012, pp. 1267–1273.
- [27] R. Kang, E. Guglielmino, D. T. Branson, and D. G. Caldwell, "Kinematic model and inverse control for continuum manipulators," in *Control and Automation (ICCA), 2013 10th IEEE International Conference on*. IEEE, 2013, pp. 1615–1620.
- [28] G. S. Chirikjian and J. W. Burdick, "A modal approach to hyper-redundant manipulator kinematics," *Robotics and Automation, IEEE Transactions on*, vol. 10, no. 3, pp. 343–354, 1994.
- [29] A. Chibani, C. Mahfoudi, T. Chettibi, R. Merzouki, and A. Zaatri, "Generating optimal reference kinematic configurations for hyper-redundant parallel robots," *Proceedings of the Institution of Mechanical Engineers, Part I: Journal of Systems and Control Engineering*, p. DOI:0959651815583423, 2015.
- [30] M. S. Espinoza, J. Gonçalves, P. Leitao, J. L. G. Sánchez, and A. Herberos, "Inverse kinematics of a 10 dof modular hyper-redundant robot resorting to exhaustive and error-optimization methods: A comparative study," in *Robotics Symposium and Latin American Robotics Symposium (SBR-LARS), 2012 Brazilian*. IEEE, 2012, pp. 125–130.
- [31] B. Karlik and S. Aydin, "An improved approach to the solution of inverse kinematics problems for robot manipulators," *Engineering applications of artificial intelligence*, vol. 13, no. 2, pp. 159–164, 2000.
- [32] Z. Bingul, H. Ertunc, and C. Oysu, "Comparison of inverse kinematics solutions using neural network for 6r robot manipulator with offset," in *Computational Intelligence Methods and Applications, 2005 ICSC Congress on*. IEEE, 2005, pp. 5–pp.
- [33] B. Daachi, T. Madani, and A. Benallegue, "Adaptive neural controller for redundant robot manipulators and collision avoidance with mobile obstacles," *Neurocomputing*, vol. 79, pp. 50–60, 2012.
- [34] A. Guez and Z. Ahmad, "Solution to the inverse kinematics problem in robotics by neural networks," in *Neural Networks, 1988., IEEE International Conference on*. IEEE, 1988, pp. 617–624.
- [35] O. Lakhal, A. Melingui, T. Morales, C. Escande, and R. Merzouki, "Forward kinematic of a class of continuum bionic handling arm," *Accepted at Robotics and Biomimetics (ROBIO), 2014 IEEE International Conference on*, 2014.
- [36] A. Melingui, C. Escande, B. Nabil, R. Merzouki, and J. Mbede, "Qualitative approach for forward kinematic modeling of a compact bionic handling assistant trunk," in *Submitted to 19th World Congress of the Int. Federation of Aut. Control, Cape Town, South Africa*, 2014, pp. 24–29.
- [37] A. Melingui, R. Merzouki, and J. Mbede, "Compact bionic handling arm control using neural networks," *Electronics Letters*, vol. 50, no. 14, pp. 979–981, 2014.
- [38] M. Arshad, T. Khan, and M. Choudhry, "Solution of forward kinematics model of six degrees of freedom parallel robot manipulator," in *Emerging Technologies, 2005. Proceedings of the IEEE Symposium on*. IEEE, 2005, pp. 393–398.
- [39] S. Haykin, *Neural networks: a comprehensive foundation*. Prentice Hall PTR, 1994.
- [40] K. Hornik, M. Stinchcombe, and H. White, "Multilayer feedforward networks are universal approximators," *Neural networks*, vol. 2, no. 5, pp. 359–366, 1989.
- [41] T. Mahl, A. Hildebrandt, and O. Sawodny, "A variable curvature continuum kinematics for kinematic control of the bionic handling assistant," *Robotics, IEEE Transactions on*, vol. 30, no. 4, pp. 935–949, 2014.
- [42] W. Wu, H. Shao, and Z. Li, "Convergence of batch bp algorithm with penalty for fnn training," in *Neural Information Processing*. Springer, 2006, pp. 562–569.
- [43] C. Escande, T. Chettibi, R. Merzouki, V. Coelen, and P. P. M., "Kinematic calibration of a multisection bionic manipulator," *Mechatronics, IEEE/ASME Transactions on*, vol. 0, no. 0, pp. 0–0, 2014.
- [44] B. A. Jones and I. D. Walker, "Practical kinematics for real-time implementation of continuum robots," *Robotics, IEEE Transactions on*, vol. 22, no. 6, pp. 1087–1099, 2006.
- [45] C. Duriez, "Control of elastic soft robots based on real-time finite element method," in *Robotics and Automation (ICRA), 2013 IEEE International Conference on*. IEEE, 2013, pp. 3982–3987.
- [46] A. Melingui, "https://www.youtube.com/watch?v=Ssgae1qJ48E," 2014.



Othman LAKHAL received the Diploma of engineer in automation and electrical engineering from the University of Lille 1, France, in 2013. He is currently a PhD student in the CRISTAL laboratory of the University of Science and Technology of Lille 1, France. His research interests include modeling, identification, and control of mobile robots and continuum manipulators.



Achille MELINGUI received the Ph.D. degree in automation and industrial computing from the University of Science and Technology of Lille 1, France, in 2014. He is currently a Lecturer in the Department of Electrical and Telecommunications Engineering at the École Nationale Supérieure Polytechnique of the University of Yaoundé I in Cameroon. His research interests include modelling and control of mobile robots and continuum manipulators, Neural Networks, and Fuzzy Logic.



Rochdi MERZOUKI received the Ph.D. degree in robotics and automation from the University of Versailles, Versailles, France, in 2002. He is currently a Professor of control and automation with the laboratory CRISTAL UMR-CNRS 9189 at Polytech' Lille, University of Science and Technology of Lille, Villeneuve d'Ascq, in France. His research interests include system of systems, modeling, and supervision of mechatronics systems applied to robotics and intelligent transport. He is the author of many contributions published in journals, conferences and books (<http://www.mocis-lagis.fr/membres/rochdi-merzouki/>). He is project manager of EU project InTraDE, www.intrade-nwe.eu.